MTF resolution of images obtained without an acquisition system

Giulio Fanti, Roberto Basso
Department of Mechanical Engineering, University of Padua,
Via Venezia 1, 35137 Padua - Italy, giulio.fanti@unipd.it, www.dim.unipd.it/fanti

ABSTRACT

The present paper proposes an extension of the traditional evaluation of the MTF curves in the case in which the acquisition system is not available and the input is not well known, if a relatively low quality of the result is accepted. The method is at first applied when only the acquisition system is unknown, and then when also the input is not well known; in this case the face and the right hand of the Turin Shroud are studied underlining the relatively high resolution of such images in comparison with other examples.

The method is applied to images of the Turin Shroud and to images obtained both by means of PP (Psychic Photography) and BEO-GDV (Biological Emission and Optical radiation - Gas Discharge Visualization). While the resolution of the Shroud images reaches *4.9±0.5 mm* at the *5%* MTF value, that of PP image is only *12±2 mm*, but the resolution of BEO-GDV images of *5.3±0.3 mm* is compatible with that of the Shroud images.

It results an anomaly at the low spatial frequencies (less than about *20* m^{-1}) that clearly presents values less than the unity. If verified with future studies, this data would set a new interesting characteristic of the Shroud image: the "acquisition system" should be characterized by the fact that the spatial frequencies around *30* m^{-1} are better represented than the others.

1. INTRODUCTION

MTF[1,2,3] curves (Modulation Transfer Function [or better its absolute value] where "modulation" is synonym of "contrast" in optics) are also named SFR (Spatial Frequency Response) and they are the mean to characterize photographic objectives and other optical systems. They are experimentally determined by comparison of input reference images with the optical output of the same image, acquired by means of the system under investigation.

From a metrological point of view optical modulation (or contrast) corresponds to resolution (also named definition) and it is the attitude to resolve details in a photographic image; in other words resolution indicates the level of details contained in an image. For example Figure 1 shows two images concerning the same input, but acquired with two different optical systems, and the corresponding MTF curves. The image on the left has clearly best resolution because its details are better reproduced: in terms of MTF curve, this image contains higher spatial frequencies that the image on the right.

MTF plots are used to characterize photographic objectives and they are obtained by the comparison of optical targets with the corresponding acquired images. With this study the standard procedure is generalized also extending it to cases in which the optical acquisition system is not available in laboratory; this is the case for example of old photos or of paintings.

As it is shown in Figure 2, the scheme of the standard procedure consists on the characterization of the acquisition system by determining its MTF curve, that is the absolute value of the ratio between the FT (Fourier Transform) of the output and input images. In this case it is necessary to have the input image and the acquisition system capable to furnish a corresponding output image.

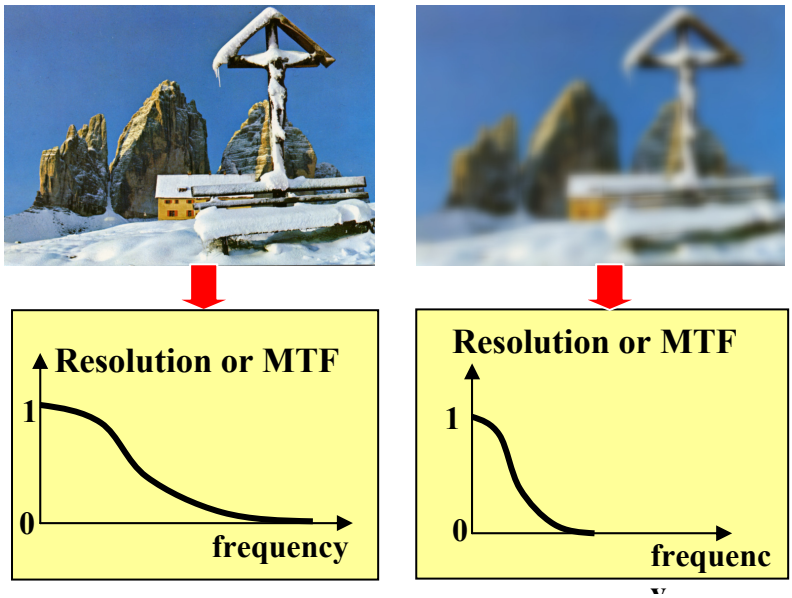

Figure 1. Two different images of the same input acquired with two different optical systems. The image on the left has a higher resolution than that on the right because it contains more details; on the bottom, the corresponding qualitative MTF curves show the different content of spatial frequencies.

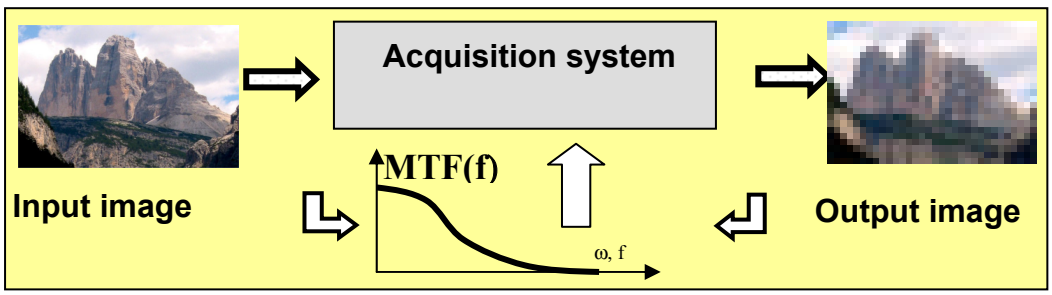

Figure 2. Scheme of the MTF standard procedure for the characterization of optical systems.

In this study instead the MTF curve will be obtained, even if characterized by a higher uncertainty, also if the acquisition system is not available; if it is not possible to have also the input image, it can sometimes be reconstructed with an approximation.

In some cases as that of the TS (Turin Shroud) also the input image is not completely known because only the output (body image impressed on a linen cloth) is detectable with its general features (young man with beard and moustaches, long hair and hardly wounded to death).

The TS face and hands will be here considered because their spatial resolutions moved some discussions in the past also in reference to the body image formation[4]. It is well known that the science is not yet able today to explain the body image formation process which presents many peculiar characteristics impossible to reproduce at same time in laboratory[5]; information correlated to the metrological characteristics of the image could help in the comprehension of the phenomenon.

The most reliable hypothesis of image formation makes reference to a burst of energy, probably connected to corona discharge[6], but other hypotheses still exists, among them that of the gas diffusion emitted by the corpse[7] or the contact process caused by body fluids[8].

One point in discussion is the resolution of the TS image because it is well known that normal radiations and gas diffusion can produce very low-resolution images (of the order of centimeters) when collimated radiations produce higher-resolution images like that of the TS. It is interesting to confirm which is the maximum resolution of the TS body image to eventually exclude some hypotheses.

After the presentation and the discussion of the proposed method for the image resolution determination, the present study applies this technique to some TS image areas rich of details such Face and Hands, and it compares the results with those obtained using other imaging techniques.

2. RESOLUTION OF IMAGES BY MEANS OF MTF CURVES

Consider an image made up of a series of black and white vertical lines characterized by an increasing spatial frequency along the horizontal direction. Depending on the acquisition system, this image can be reproduced in a photograph with higher or lower level of resolution. Two different types of acquisition systems, capable to acquire different details or different spatial frequencies of the image shown up in the background in the example of Figure 3 are shown.

Object of the present paper is the quantification of the resolution of the acquired images.

2.1. THE MTF FUNCTION

The bidimensional transfer function[8] $h(x,y)$ is defined as the ratio between output $g(x,y)$ and input $f(x,y)$ which represent the image luminance. The output is given in the 2-D space domain by the convolution of input with the transfer function:

$$g(x,y) = \int_{-\infty}^{+\infty}\int_{-\infty}^{+\infty} f(x_1,y_1)h(x-x_1,y-y_1)dx_1dy_1 \qquad \textit{(Eq. 1)}$$

If $h(x,y)$ is determined as the result of an input image corresponding to the δ function (Dirac), it is called $PSF(x,y)$ (Point Spread Function):

$$PSF(x,y) = h(x,y) \qquad \textit{(Eq. 2)}$$

Being respectively $H(f_x, f_y)$, $G(f_x, f_y)$ e $F(f_x, f_y)$ the bidimensional FTs of $h(x,y)$, $g(x,y)$ and $f(x,y)$, and f_x, f_y the spatial frequencies along the x e y directions, it results:

$$H(f_x,f_y) = \frac{G(f_x,f_y)}{F(f_x,f_y)} = MTF(f_x,f_y) \cdot e^{i\varphi(f_x,f_y)} \qquad \textit{(Eq. 3)}$$

$H(f_x, f_y)$ is also called OTF (Optical Transfer Function) and its absolute value is the MTF, as the phase difference is generally negligible at the lower frequencies of interest:

$$\left|H(f_x,f_y)\right| = \left|OTF(f_x,f_y)\right| = MTF(f_x,f_y) \qquad \textit{(Eq. 4)}$$

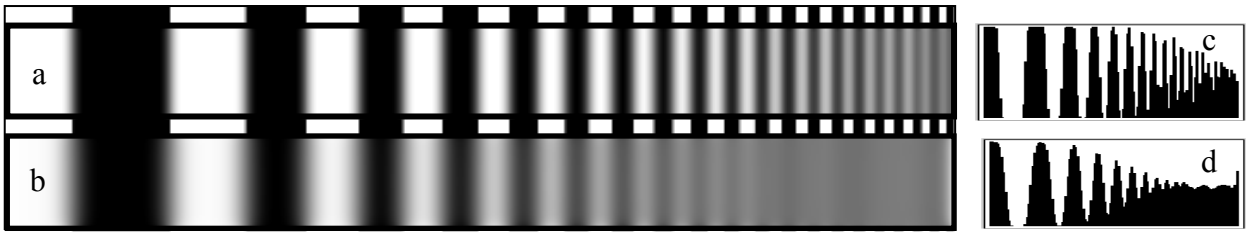

Figure 3. Input image on the background, consisting in a series of black and white vertical lines having increasing spatial frequencies, from the left to the right; it has been acquired in the windows (a) and (b) using two different optical systems. The resolution of System (a) is sufficient to reproduce all the vertical lines while the System (b) is not able to reproduce vertical lines characterized by higher frequencies. This fact is evidenced in windows (c) and (d) that shows the luminance values relative to the same horizontal lines, respectively of window (a) and (b). The aliasing effect can also be observed in system (b) just under the letter "d".

2.2. RESOLUTION OF IMAGES

From Eq.s (3) and (4) the $MTF(f_x, f_y)$ results defined as:

$$MTF(f_x,f_y) = \left|\frac{G(f_x,f_y)}{F(f_x,f_y)}\right| \qquad \textit{(Eq. 5)}$$

In a digital image having m x n pixels of the same dimensions, the $MTF(f_x, f_y)$ is given by the luminance values ratio of the FTs respectively of the output and input images. It must be noted that the upper spatial frequency is equal to half the inverse of the pixel dimension and that the spatial frequency resolution is equal to the inverse of the total image dimension, both evaluated along the considered direction.

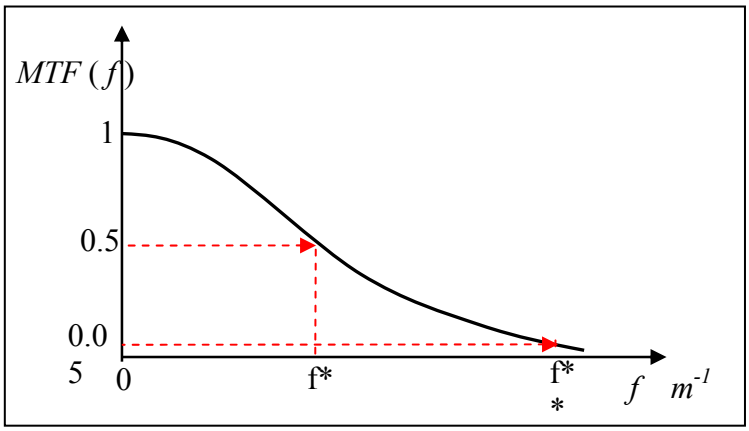

Figure 4. Example of MTF (f) curve where the image resolutions at 50% and 5% respectively of the spatial frequencies f ed f** are shown.*

The MTF characterizes the spatial resolution of the image in the spatial frequency domain along a predefined direction. The MTF curves, relative to a specific direction, are represented in Cartesian plots where the abscissa is the spatial frequency f (or pairs of lines per unit length) measured in m^{-1} and the ordinate is the corresponding *MTF(f)* value between *0* and *1*, see Figure 4.

It must be noted that the image details depend on the higher frequencies reproduced in it, therefore the best acquisition system should have a constant transfer function equal to *1*.

If not differently specified, we make reference to the resolution corresponding to an output/input ratio of *5%* in this paper, see Figure 4, because optical information of the image under analysis begins to disappear to the sight beyond this limit. We also make reference to the resolution corresponding to the *50%* because this value is significant for the optical systems characterization such as photographic objectives.

If f^* is the value corresponding to $MTF(f^*)=0.5$, and f^{**} is the value corresponding to $MTF(f^{**})=0.05$, all the frequencies equal or lower than respectively f^* and f^{**} are reproduced in the output image with details equal or better than *50%* and *5%* of those of the input image. As the details having frequencies greater than f^{**} are not easy to distinguish, they are considered negligible.

2.3. EXAMPLE

An image having a sinusoidal shape along the x-axis is considered as input, see Figure 5; along the horizontal direction we have:

$$f(x) = a + b \cos(2\pi f' x) \qquad \text{(Eq. 6)}$$

where the frequency $f' = \omega/2\pi$ corresponds to the number of cycles per unit length (or to the number of black/white lines couples contained in a meter). The input modulation M_i and the output one M_o are respectively:

$$M_i = \frac{f(x)_{\max} - f(x)_{\min}}{f(x)_{\max} + f(x)_{\min}} \; ; \quad M_u = \frac{g(x)_{\max} - g(x)_{\min}}{g(x)_{\max} + g(x)_{\min}} \qquad \text{(Eq. 7)}$$

where $f(x)_{max}$, $f(x)_{min}$ are respectively maximum and minimum luminance values of the input image and $g(x)_{max}$, $g(x)_{min}$ those of output image. If $f(x)$ is given by Eq. (6), we have $M_i = b/a$ and, using Eq. (5), $M_u = MTF(f)\ b/a$.

If the image shown in Figure 5 is acquired with *256* grey levels, and at the spatial frequency *f'* we have $f(x)_{max}=180$ and $f(x)_{min}=20$; using Eq. (7) it results:

$$M_i=0.8.$$

If at the same spatial frequency *f',* we have $g(x)_{max}=140$ and $g(x)_{min}=60$, it results:

$$M_u=0.4.$$

Using Eq. (5), the MTF curve of the system in correspondence of *f'*, gives then:

$$MTF(f')=0.5$$

This also means that the spatial frequency *f'* corresponds to *f** because at that frequency, the acquisition system reduces the input signal amplitude by a factor *0.5*.

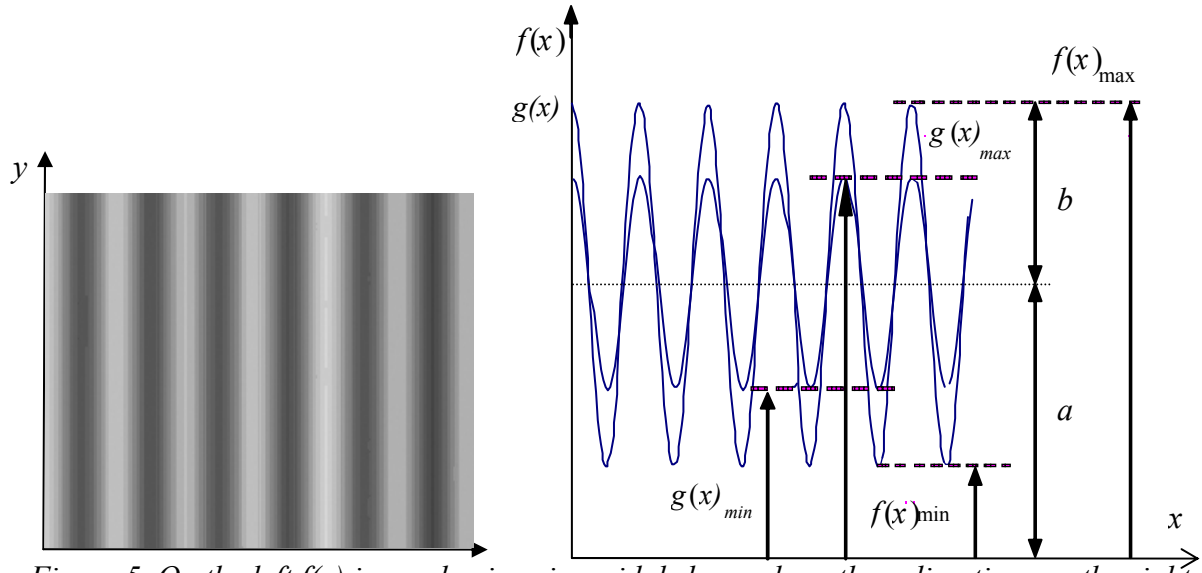

Figure 5. On the left f(x) image having sinusoidal shape along the x direction; on the right luminance values plot along an horizontal line of f(x) image and corresponding output g(x).

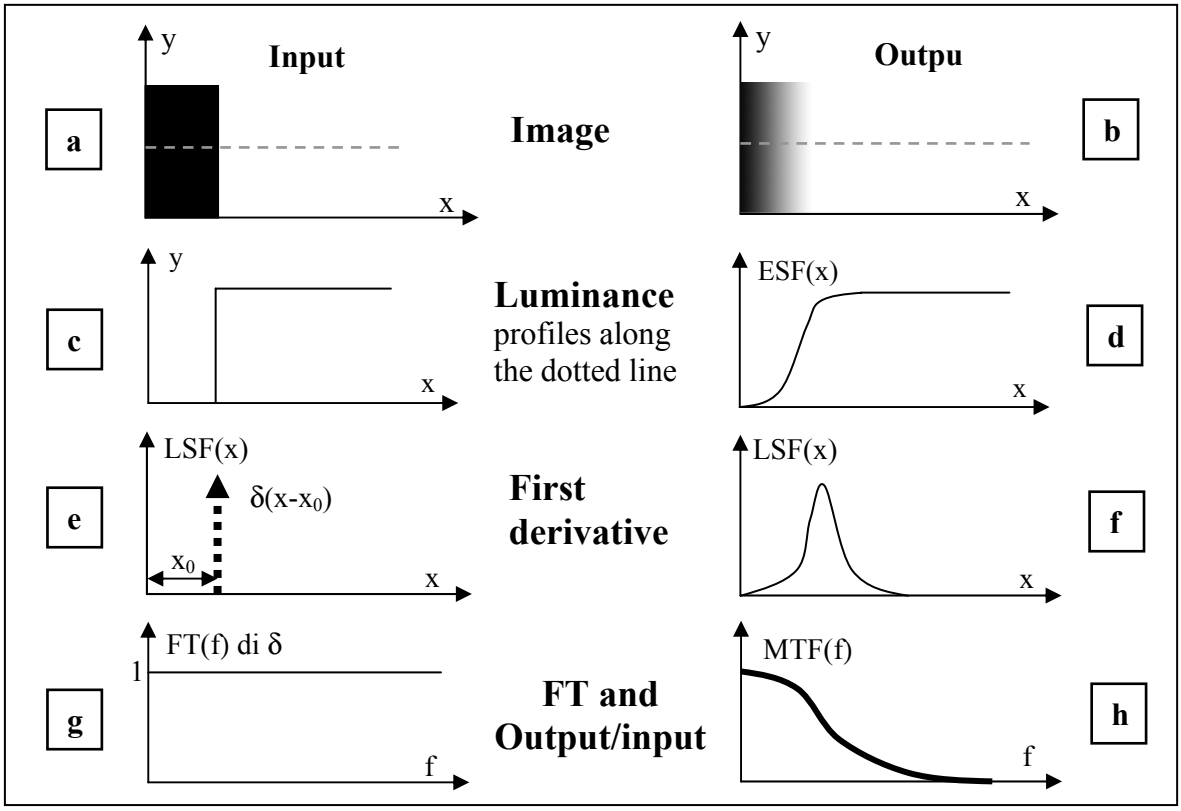

Figure 6. EET different phases. -1) The image of a step function is acquired, obtaining the output of the optical system under investigation (b). -2) The corresponding luminance levels along the dotted line are evaluated (c, d) obtaining the ESF. -3) The first spatial derivative (e, f) are calculated obtaining the LSF because the first derivative of the Heaviside function is the Dirac function $\delta(t)$. -4) The FT of a unit impulse $\delta(t)$ gives a flat spectrum of amplitude 1(g) and the transfer function of the optical system (h) is the FT of the LSF (f).

3. THE EDGE EXPOSURE TECHNIQUE

The system transfer function can be obtained by means of the EET (Edge Exposure Technique) processing the image obtained by an optical system that acquires a step function called ESF (Edge Spread Function). Using its first derivative, the LSF (Line Spread Function) is obtained.

The FT of LSF furnishes the transfer function according to the procedure described in Figure 6.

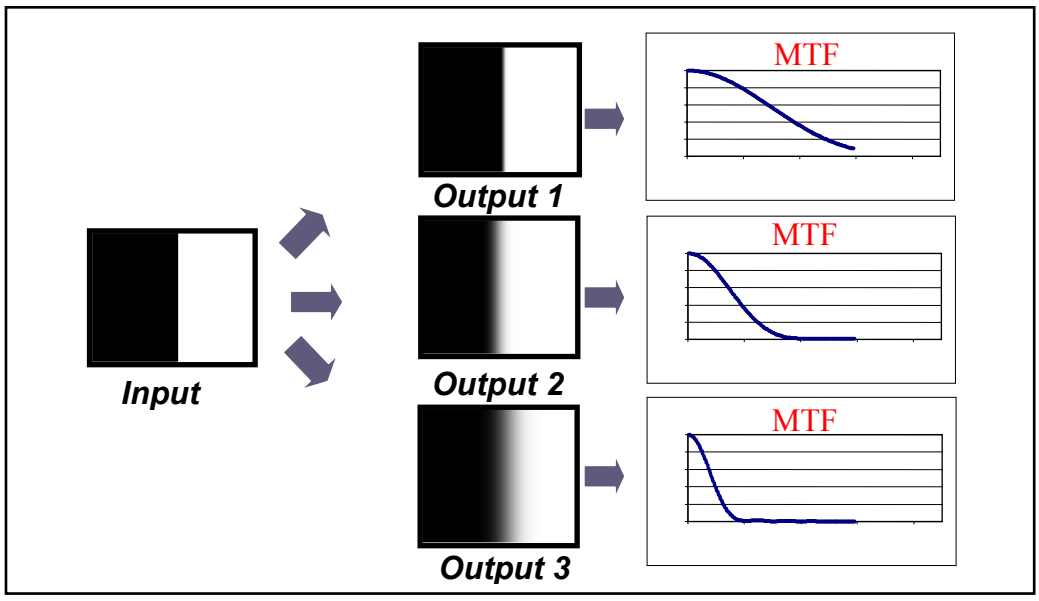

Figure 7. Example of EET: effect of three different acquisition systems on MTS curves.

4. MTF EVALUATION IN THE ABSENCE OF THE ACQUISITION SYSTEM

The traditional methods for the evaluation of MTF curves are not applicable if we do not have the acquisition system, and more less if the input image is absent. If the acquisition system is absent, the image can be photographed and digitized, in the hypothesis that the photographic system has a resolution better at least three or four times with respect that of the subject to be studied.

Instead, it is not correct to analyze only the FT of the output image and to correlate it to an MTF curve, because the subject reproduced in the image is not characterized in general by a not uniform content in spatial frequencies as it is requested in the application of the EET.

In absence of the input image, one or more subjects very similar to the one represented in the image under exam are chosen, and they must be photographed in conditions as similar as possible. The bi-dimensional FT of the assumptive inputs are therefore calculated and, after a possible average of the resulting values, the Eq (5) is applied to determine the MFT and then both the output image resolution and the characteristics of the unknown acquisition system.

The proposed method consists in the following steps:

1. Input and output image digitalization.
2. Calculation of the 2-D FT of the two images to determine the relative spectra muduli.

Noise reduction above all if the image under analysis has also spatial frequencies not typical of the reproduced image (as it is the case of weft background of fabrics).

3. Analysis of the pixels luminance along the lines of interest.
4. Construction of the MTF curves for the resolution evaluation along the lines of interest.

A preliminary feasibility analysis on well-known samples (vertical lines) has shown the method applicability. Therefore we proceeded applying the method to experimental images obtained by a system of unknown acquisition characteristics. In particular, photographs of images of objects obtained on flax clothes using a special technique[7] which is based on the

diffusion of reactive gases produced by evaporation from objects of several forms, have been analyzed. The technique has been then applied to the TS body image, see Figure 8, where neither the acquisition system nor the details of the input image are known.

Therefore in this case the details of the TS face and hands have been compared with those photographed in as similar as possible conditions. A reproducibility analysis has been performed on these images using different inputs. For comparison the technique has been also applied to images obtained by other experiments.

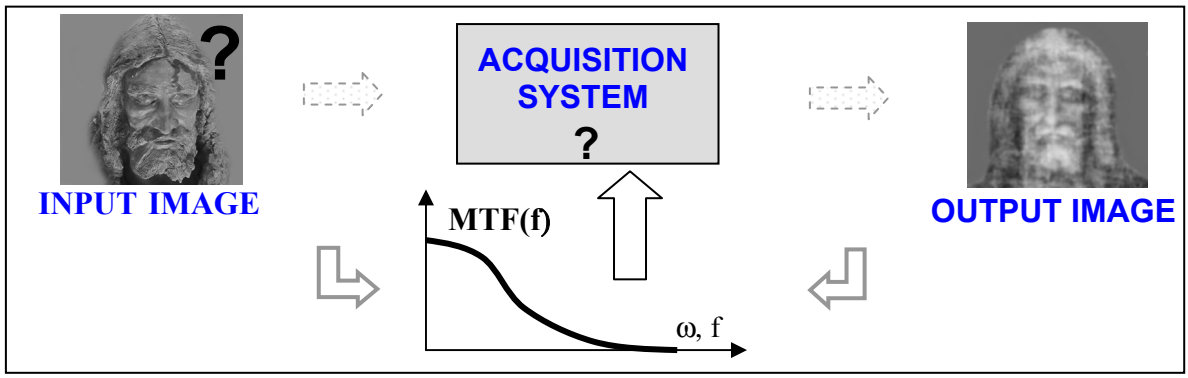

Figure 8. Scheme of the proposed technique in the case of both input and acquisition system not known, to be compared with the standard technique of Figure 2.

4.1. TECHNICAL SPECIFICATIONS

All the images have been acquired and processed according to the specifications below reported in order to be compared among each other. Photographs have been acquired with photographic systems characterized by MTF curves at least 3-4 times better than the curves relative the images of interest, and therefore the influence of the used photographic system on the results is considered as negligible.

Input images have dimensions greater than *256x256* pixels so that they must be definite in windows of *256x256* pixels (or multiples) on which perform both the direct FT (to analyze their frequency content) and the inverse one (to check the result in the space domain after eventually having removed frequencies associated with possible noise)[6].

Pixels dimension are $l_p = 0.5\ mm$. In case of images of lower dimensions, as the case of the threads presented in § 5, the analyzed image consists in the composition of several copies of the same detail (two in the horizontal direction and two in the vertical direction). To obtain this condition, an image resizing has been carried out with uncertainty of the order of 3%. Therefore the dimensions of the analyzed windows of 256x256 pixels are *12.8 cm x 12.8 cm*.

The upper frequency f_{up} results:

$$f_{up} = \frac{1}{2L_p} = \ 1000 \ \ m^{-1} \qquad \textit{(Eq. 8)}$$

The spatial frequency resolution Δf, along the x and y axes, results:

$$\Delta F = f_p / 256 = 3.90625\ m^{-1} \qquad \textit{(Eq. 9)}$$

while, being square the pixel, it results $\Delta F = 5.524 \pm 5\%\ m^{-1}$ in the direction inclined of 45° with respect to the axes (image of the thread), and $\Delta F = 4.638 \pm 5\%\ m^{-1}$ in the direction inclined of 58° (image of the hands).

To reduce the noise effects in frequency spectra, we proceeded in various ways:

-a) in the case of face input image, the averages of the spectra concerning different input images were performed, after executing the average of four spectra relative to various positions of the acquisition windows in the image;

-b) before to make the FT, the frequency content of interest information has been made clear, trying to remove the frequency content correlated to the noise[6]. For instance, canceling particular frequencies by means of direct and inverse FTs, we highlighted the frequencies relative to noise and to the fabric weft; other noises have been as well removed with opportune Gaussian blurring;

-c) FT Spectrum peaks have been smoothed performing a Gaussian blur having 2 pixels radius;

-d) the images have been equalized and the backgrounds have been made as much as possible uniform before executing the FTs.

Through Optimas 6® software, the luminance profiles have been extracted along the directions of interest; these numerical values have been processed with KaleidaGraph® software to obtain the corresponding MTF curves. All the images representing the FT have been corrected with a gamma value equal to *5* to better to highlight the luminance variations. In the processed images, the position of the window of *256 x 256* pixels, where the FT was applied, is highlighted.

The uncertainty analysis of the MTF curves, that afterwards will be referred with a level of confidence of *95%*, has highlighted as primary source the reproducibility of procedure: a shifting of the window of interest of about ten of pixels in the image under analysis in fact causes local luminance value changes also greater than *20%*. An uncertainty of *±5%* to the MTF curve, resulting from the average of different FTs, has been therefore assigned in the case the input image was known.

In the case the input image was unknown, the uncertainty model caused a further contribution, that combined with the reproducibility uncertainty, led to an assignment of at least *±10%* to the MTF curve, resulting from the average of more FTs. From the result of several tests in various conditions, where the MTF curve have turned out less reproducible, the uncertainty value has been increased, in accordance with the resulting plots reported in the next sections.

5. MTF RESULTS IN THE ABSENCE OF THE ACQUISITION SYSTEM

It is also possible to obtain images of objects through non photographic techniques; this is the case of paintings, and when an image is recorded on a surface using special techniques. For instance it is known that the leaves, pressed in the herbariums, after a particular time period, leave fixed their image on the paper sheets in contact with them.

Another example, see Figure 9, is given by the image which can be obtained on a fabric soaked in sugary substances and later dried finally placed near cords impregnated with amino substances.

It is interesting in this case to know the resolution of the resulting image in comparison with that of the TS, because some researchers think that the body image on the TS can have formed by a similar diffusive[7] process.

In this case we have the photograph of the input image, see Figure 9a, and that of output, but it is not easy to perform a direct calibration of the "acquisition system" consisting in the diffusive mechanism of the gases given off from the cords which react with the fabric. The Figures 9 (b, d)

respectively report the bi-dimensional FT of the images shown in the Figures 9 (a, c): the prevailing development of the two FTs in the direction inclined of 45° is observed since the cords are almost rectilinear and inclined of -45°.

Applying the Eq. (5), the MTF curve of the image of Figure 9c, calculated along the inclined direction of 45° is obtained in Figure 10. Assigned a minimum uncertainty of ± 0.05 to the MTF curve, the characteristic frequencies are:

$f^* = 21 \pm 3\ m^{-1}$ corresponding to $MTF\ (f^*) = 0.5$;

$f^{**} = 57 \pm 17\ m^{-1}$ corresponding to $MTF\ (f^*) = 0.05$.

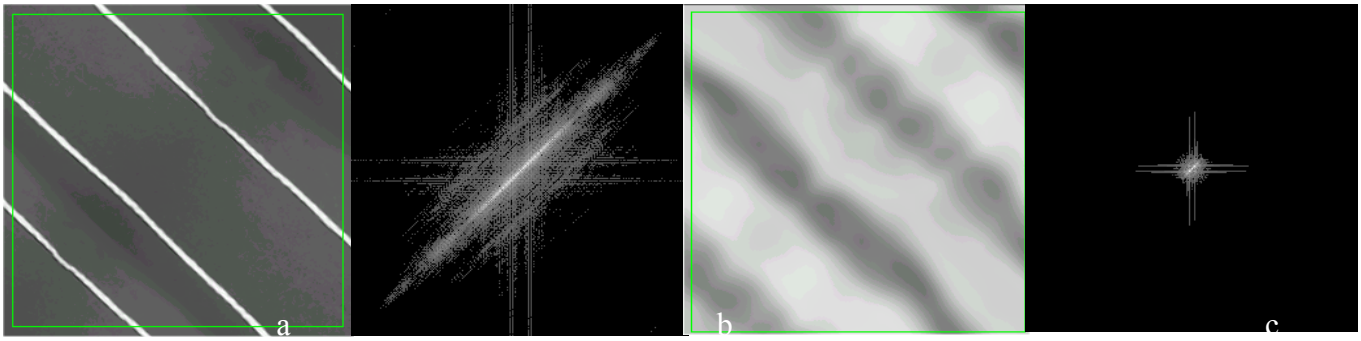

Figure 9. a) Input image of cords (courtesy of Ray Rogers); b) FT of image (a); c) output image of cords on a fabric (courtesy of Ray Rogers); d) FT of the image (c).

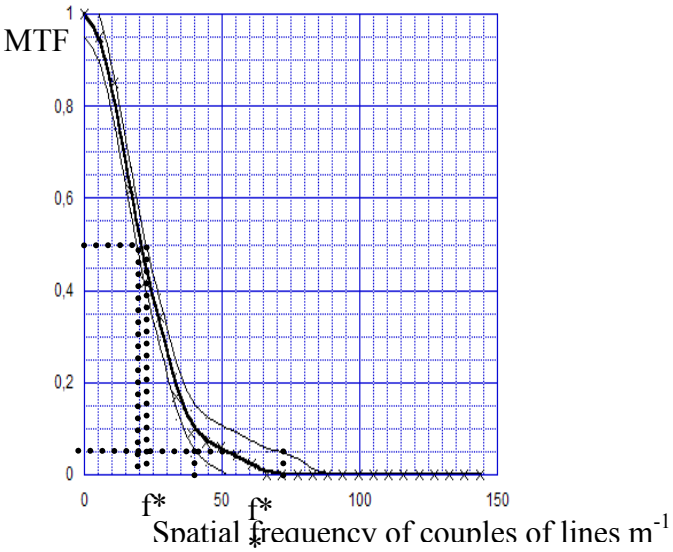

Figure 10. MTF curve of the images of Figures 9 calculated along the 45° direction.

It must be reminded that is not always possible to obtain acceptable images from every object using the diffusion technique just tested. This is the case of the images of a pine-cone (Figure 11) or of a human hand made using packed newspapers (see Figure 12), both obtained in the same way of the cords of Figure 9.

The resulting images of pine-cone and of newspapers - human hand are characterized by such a low resolution that the MTF technique gave no measurable results. This means that the resolution of these images is worse than at least a factor 10 with respect to the results regarding the cords.

Because of the low resolution levels reached with this technique, the related hypothesis of the TS body image formation by means a gas diffusion mechanism is not worth of consideration.

Figure 11. A pine-cone as input image; in the photo it was leaned on the fabric having impressed the corresponding output image (courtesy of Ray Rogers); in this case the resolution of the output image is so low that no reliable MTF curves can be obtained.

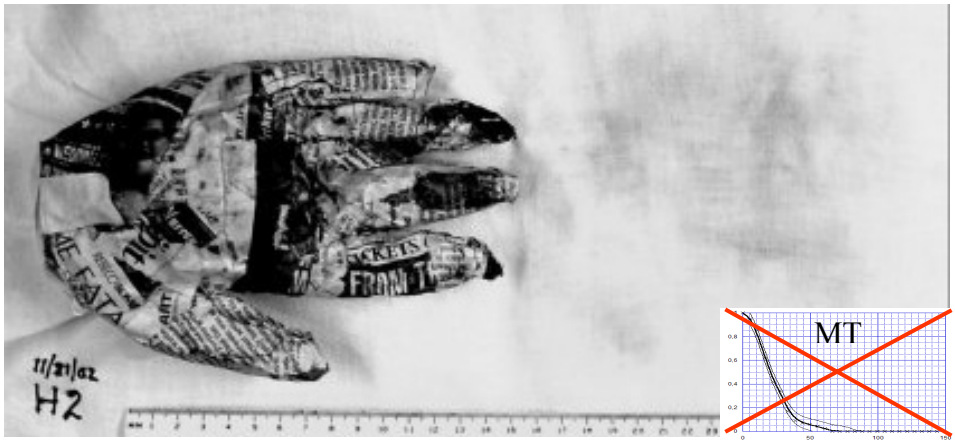

Figure 12. An human hand made with packed newspapers as input image; in the photo it was leaned on the fabric having impressed the corresponding output image (courtesy of Ray Rogers); also in this case the resolution of the output image is so low that no reliable MTF curves can be obtained.

6. MTF RESULTS IN THE ABSENCE OF THE ACQUISITION SYSTEM WHEN ALSO THE INPUT IMAGE ARE NOT WELL KNOWN

In case of depictions and images reproduced by means of different techniques, it can be interesting to have technical information, even if of reduced quality, on the output image, also in the cases in which both of the acquisition system and the exact input image are not known. For example the MTF technique could be applied in the characterization of the "painter hand" in some painting of doubtful origin.

The TS image, which has woken up discussions in reference to its explanation and also to its resolution, is considered in this work as an applicatory example. The relatively high content in spatial frequency of such an image will be then compared with the resolution obtained through other acquisition systems.

6.1. ANALYSIS OF FACE

To perform the TS face analysis, Figure 13, it has been necessary to provide photographs of faces like that of the TS to be used as input images.

The photographs of two sculptures, and that of a person with the long hair, beard and moustache have been chosen; of such images the average of the corresponding 2-D FT has been considered, Figure 14.

With the application of Eq (5), the MTF curve of the image of Figure 13a, calculated along the vertical direction (to highlight the spatial frequencies concerning the mouth and the eyebrows), is obtained in Figure 15.

Once assigned a minimum uncertainty of $\pm\ 0.1$ to the MTF curve, greater than in the case of the cords because in this case the input image is not perfectly known, the characteristic frequencies are:

$f^* = 39 \pm 13\ m^{-1}$ corresponding to $MTF\ (f^*) = 0.5$;
$f^{**} = 101 \pm 9\ m^{-1}$ corresponding to $MTF\ (f^{**}) = 0.05$.

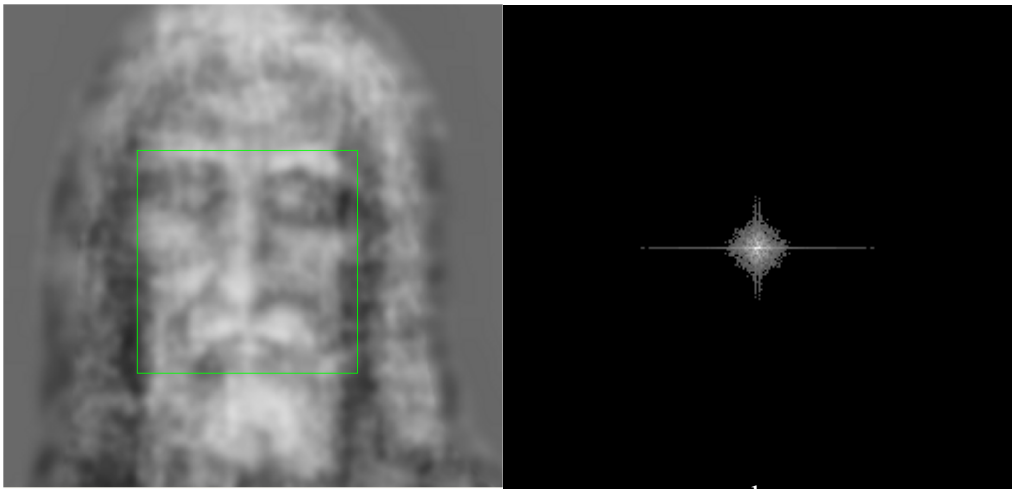

Figure 13. a) TS Man Face cleaned up by various noises such as the blood stains and the fabric weft; b) FT of image (a).

Figure 14. a) Erick Erickson sculpture photograph; b) Luigi Mattei sculpture photograph; c) average of the FT of various images like the TS.

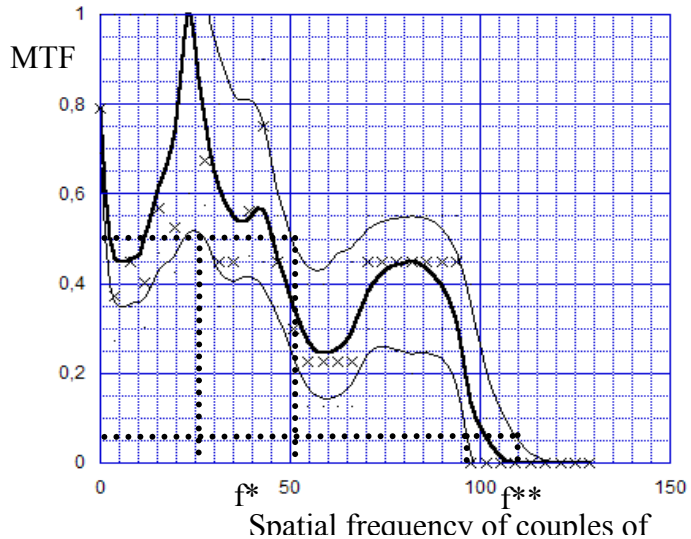

Figure 15. MTF curve of TS face evaluated along the vertical direction.

The MTF curve of a face obtained through another technique called PP (Psychic Photography[9]) has been calculated for comparison, see Figure 16. Figure 17 which shows the MTF curves of the TS face (a) and of the one concerning the PP acquisition (b), along the inclined direction of 45°, highlights the best resolution regarding the TS image.

Once assigned a minimum uncertainty of ± 0.10 to the MTF curves, the characteristic frequencies are:

for the TS image (Figure 17a)

$f^* = 22 \pm 7\ m^{-1}$ corresponding to $MTF(f^*) = 0.5$;

$f^{**} = 85 \pm 9\ m^{-1}$ corresponding to $MTF(f^{**}) = 0.05$

and for the PP image (Figure 17b)

$f^* = 7 \pm 4\ m^{-1}$ corresponding to $MTF(f^*) = 0.5$;

$f^{**} = 42 \pm 6\ m^{-1}$ corresponding to $MTF(f^{**}) = 0.05$.

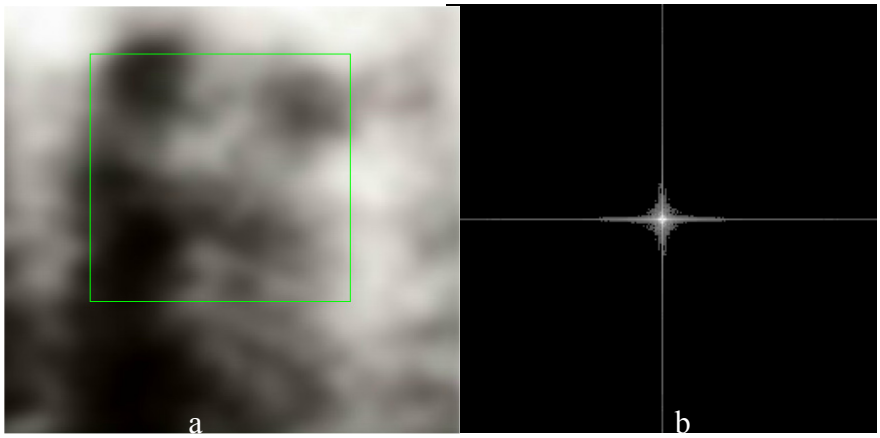

Figure 16. a) Face obtained through the PP technique (S. Benford); b) FT of (a).

It results what follows:

-a) The resolution values of the TS image, evaluated along the vertical direction, are compatible with the ones evaluated at 45°. Nevertheless along this direction the lower resolution could be caused by the shortage of spatial information with respect to the

information contained in the vertical direction (lips and eyebrows). In any case the MTF analysis of another TS detail rich of information, the image of the TS hands, is then performed, to verify the previous results.

-b) The resolution of the face obtained with the PP technique is at least less 2 times worse than that of the TS image.

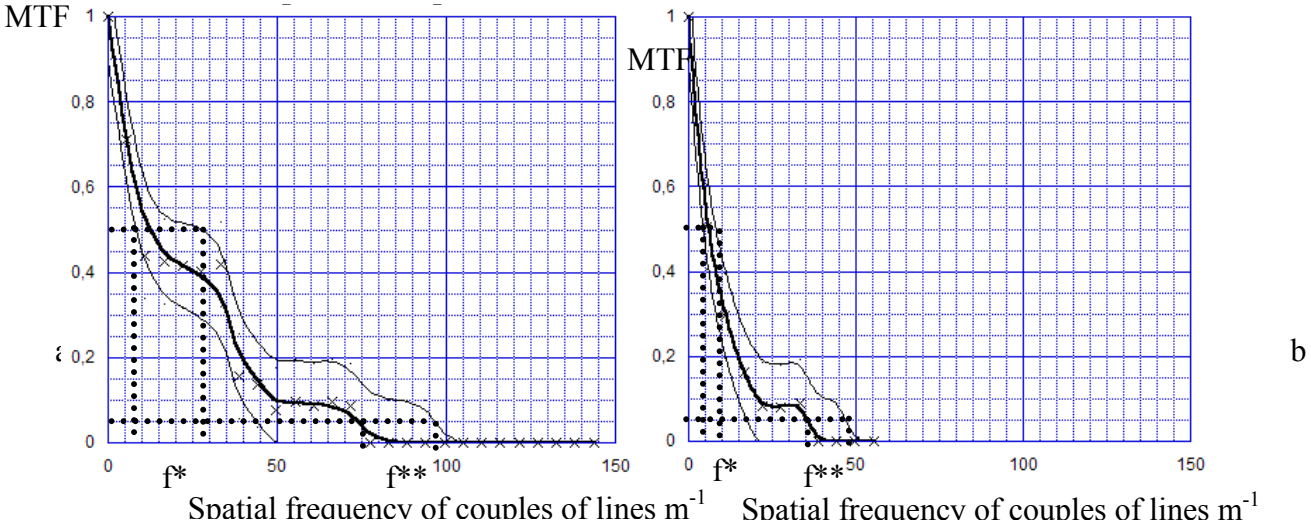

Figure 17. MTF curve of faces calculated along the inclined direction of 45° of (a) TS; b) PP experiment.

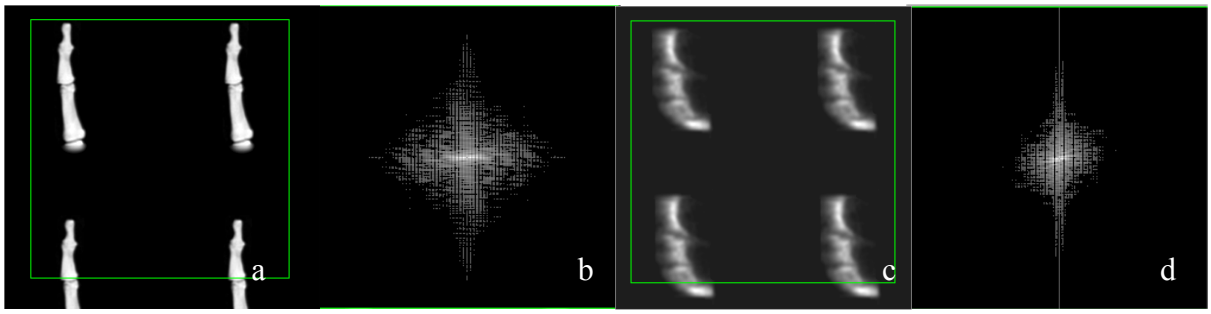

Figure 18. a) Input image of the pinkie finger; b) FT of image (a); c) output image of the pinkie finger obtained with technique BEO-GDV[10, 11] (S. Benford); d) FT of the image (c).

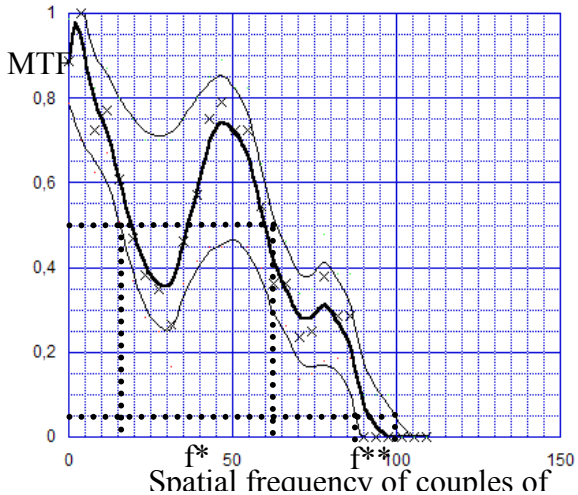

Figure 19. MTF curve of the pinkie finger calculated along the horizontal direction: BEO-GDV experiment.

For comparison, the evaluation of the MTF of the image of a pinkie finger obtained using the technique BEO-GDV (Biological Emission and Optical radiation, Discharge Visualization gas)[10, 11] (a technique used in the clinical diagnostics to highlight tumor presences) is shown up, see Figure 18. The Figure 19, showing the MTF curve of the pinkie finger BEO-GDV image (along the horizontal direction) highlights a resolution comparable to that of the TS image.

Assigned a minimum uncertainty of ± 0.10 to the MTF curve, the characteristic frequencies are:

$f^* = 39 \pm 23\ m^{-1}$ corresponding to $MTF\ (f^*) = 0.5$;
$f^{**} = 94 \pm 6\ m^{-1}$ corresponding to $MTF\ (f^{**}) = 0.05$.

6.2. ANALYSIS OF THE TS HANDS

The MTF analysis of the TS image has been performed also in correspondence of the hands; the respective 2-D FT of the input image of figure 20a, and that of the TS hands of Figure 20c are shown in the Figures 20 (b, d). The prevailing development of the two FTs along the direction inclined of 58° is observed, since right hand fingers are inclined of -32° in the image.

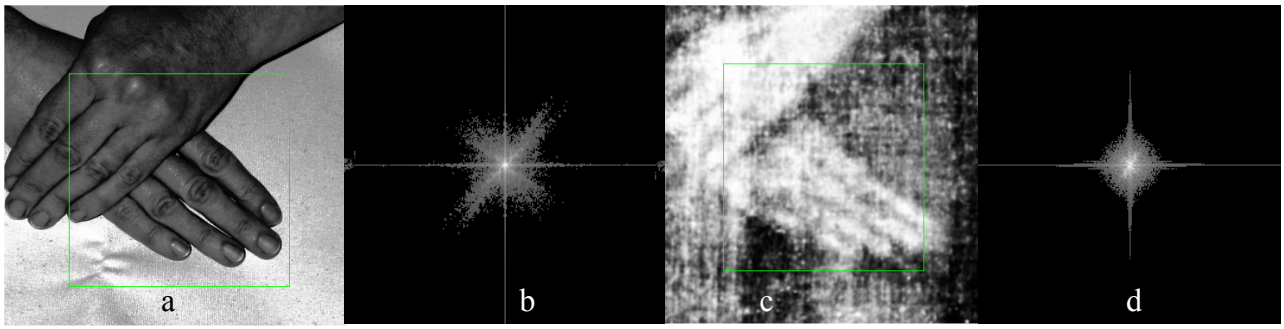

Figure 20. a) Input image; b) FT of image (a); c) output image; d) FT of the image (c).

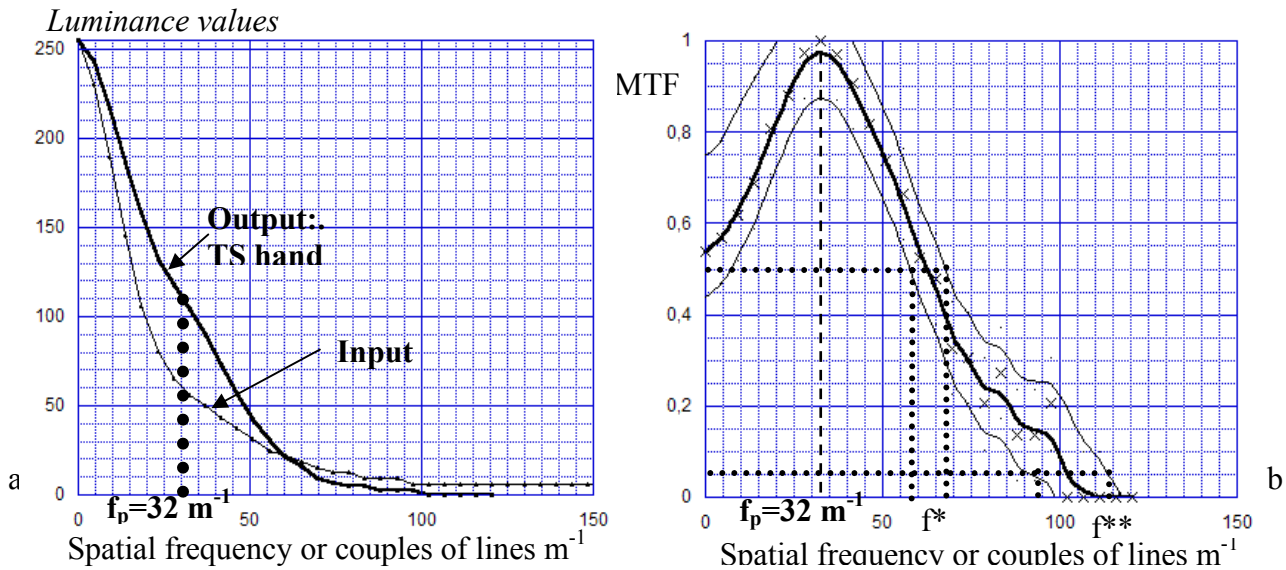

Figure 21. -a) equalized luminance profiles of the images of figure 20 (b, d) evaluated starting from the image center in direction of 58°; -b) curve MTF of TS right hand: we observe the peak at the frequency $f_p = 32\ m^{-1}$ probably typical of the TS image.

The luminance levels of input and output images of Figure 20 (b, d) are shown in Figure 21a. Applying the Eq. (5) we obtain the MTF curve of the image of Figure 20c, calculated along the

sloping direction of 58°, in Figure 21b. Assigned a minimum uncertainty of ± *0.1* to the MTF curve, the characteristic frequencies are:

$f^* = 63 \pm 5\ m^{-1}$ corresponding to $MTF\ (f^*) = 0.5$;

$f^{**} = 104 \pm 10\ m^{-1}$ corresponding to $MTF\ (f^{**}) = 0.05$.

7. COMMENTS

From the above analysis it results what follows.

-1) The MTF value corresponding to the frequency f^{**} of the TS right hand ($=104 \pm 10\ m^{-1}$) is compatible with that ($101 \pm 9\ m^{-1}$) of the face. Instead the MTF value corresponding to the frequency f^* of the TS right hand ($63 \pm 5\ m^{-1}$) is not compatible with that ($39 \pm 13\ m^{-1}$) of the face: the poor reliability of the results of Figure 17a, probably due to a lack of details in the inclined direction of 45°, is confirmed.

-2) Based on the results of the Figures 15 and 18b, the following MTF values are assigned to the f^* and f^{**} frequencies, taking into account that the various data could contain some systematic effect, also due to the presence of not completely removed noise, and considering that the hand image is more reliable because it contains clear details in the direction of 58°:

$f^* = 60 \pm 10\ m^{-1}$ corresponding to $MTF\ (f^*) = 0.5$;

$f^{**} = 103 \pm 10\ m^{-1}$ corresponding to $MTF\ (f^*) = 0.05$.

It is known that in case of a frequency of $100\ m^{-1}$, a couple of lines of the dimension of *10 mm* (equal to $1/100\ m^{-1}$) are perceivable.

In the case of the TS image, the resolution at the frequency $f^{**} = 103 \pm 10\ m^{-1}$ is

$R = 4.9 \pm 0.5$ *mm*

in correspondence to a contrast of *5%*.

Figure 22. 3-D processing of the TS face; some bumps having a spatial period of about 31 mm (indicated on the top as two segments) are evident. They could be typical of the TS body image formation mechanism.

-3) These results are in agreement with those of a previous work[6] in which it was stated, in a non quantitative way, that the highest characteristic frequencies of the TS face are included in the range between 80 m^{-1}, and 100 m^{-1}.

-4) The MTF curves of the Figures 15 and 21b highlight a trend unlike from the typical ones (see for example the Figures 4 and 10). In fact the peak at the frequency $f_p = 32\ m^{-1}$ is well evident. This shows that the TS image could be different from the normal images: on the TS, it would seem that the information at spatial frequencies lower than 20 m^{-1} is not well codified (lines of about *25 mm* of thickness) while the spatial frequencies of about $30\ m^{-1}$ would seem much better codified (lines of about *15 mm*). If verified, future studies addressed to the TS image formation mechanism will have to take this characteristic into account.

-5) The anomaly detected at point (3) can be supported if a 3-D processing of the TS image of face is performed. As shown in Figure 22, some bumps having a spatial period of about *31 mm* (corresponding to $f_p = 32\ m^{-1}$) there appear, and probably they correspond to a particular mechanism of body image formation.

-6) The MTF curve of the Figure 19 with reference to the BEO-GDV experiment of a pinkie finger also shows an unlike trend, and it shows that the resolution of the obtained image ($f^* = 39 \pm 23\ m^{-1}$; $f^{**} = 94 \pm 6\ m^{-1}$) is compatible with that of the TS image ($f^* = 60 \pm 10\ m^{-1}$; $f^{**} = 103 \pm 10\ m^{-1}$). Therefore only under the point of view of resolution, the BEO-GDV technique could be considered for the explanation of the TS body image.

8. CONCLUSION

The proposed method has allowed evaluating the MTF curves relative to images of which the acquisition system is not known. The method is also applicable to some cases in which the input is not known in a complete way, but the result quality is lower than the one normally obtained. The minimum uncertainty band of the curve MTF of TS face and hands is $\pm\ 0.1$.

The method applied to evaluate the MTF curve of an image produced by chemical reaction of gases exhaled by cords, furnishes a resolution at the value of *5%* of the MTF curve of the output image of $9 \pm 3\ mm$.

The method is also applied to images in which complete information about the input are absent: the face and the right hand of the TS and images obtained with PP and BEO-GDV technique. While the TS image resolution reaches $4.9 \pm 0.5\ mm$ at the 5% value of the MTF curve, that of PP images leads to $12 \pm 2\ mm$. The resolution of BEO-GDV image, resulting $5.3 \pm 0.3\ mm$, is instead compatible with that of the TS images.

From the comparison of the MTF curves relative to the TS images of the face and the right hand with the ones typical of optic systems, an anomaly has turned out which has values much lower than the unity at the low spatial frequencies (less than about $20\ m^{-1}$). If verified with future studies, this result would place a new interesting characteristic of the TS image in which the spatial frequencies in the range around $30\ m^{-1}$ are better represented than others.

These results, in reference to studies about the possible body image formation mechanism of the TS, that is not yet known to science, are in favor of a radiative phenomenon coming from the inner of the human body enveloped in the TS, they are instead contrary to the gas diffusion hypothesis as a main cause of the image formation and they are open new possibilities of comparison with the BEO-GDV technique.

REFERENCES

-1) SPIE: “Modulation Transfer Function” Society of Photo-Optical Instrumentation Engineers, Redondo Beach, California, 1968, Proceedings, Seminar-in-Depth.

-2) http://www.imatest.com/docs/sharpness.html, www.normankoren.com/Tutorials/MTF.html

-3) Nadir Magazine: http://www.nadir.it/ob-fot_miscell/valutaz_obiett.htm

-4) Fanti G., Marinelli E.: “La Sindone rinnovata – misteri e certezze” Ed. Progetto Editoriale Mariano, Vigodarzere (PD), March 2003.

-5) Moran K., Fanti G.: “Does the Shroud body image show any physical evidence of Resurrection?”, IV Symposium Scientifique International sur le Linceul de Turin, Paris, 25-26 April 2002, http://space.tin.it/scienza/bachm/MORAN2.PDF.

-6) Fanti G., Maggiolo R.: "The double superficiality of the frontal image of the Turin Shroud", Journal of Optics A: Pure and Applied Optics, volume 6, issue 6, pages 491- 503, April 2004; http://www.sindone.info/FANTI.PDF

-7) Rogers R.: http://www.shroud.com/pdfs/rogers2.pdf

-8) Volckringer J.: “The Holy Shroud: science confronts the imprints”, The Runciman Press, Manly, Australia 1991.

-8) Zattra L.: “Determinazione del modulo della funzione di trasferimento per la stima della risoluzione di immagini [Determination of the absolute value of the transfer function to esteem the image resolution]” Tesi di laurea Dip. Ingegneria Meccanica Università di Padova, relatore G. Fanti, a.a. 2003-2004.

- 9) Eisenbud J.: “The Serios 'blackies' and related phenomena” Journal of the American Society for Psychical Research, 66, 180-192(1972).; http://www.psiexplorer.com/thoughtography.htm

-10) Shaduri M., BEO-GDV: http://www.sacredoilsofkrishna.com/gdv_tech.html
http://www.fairs.ru/vist02/v_201102/thezis/thez_8e.htm

-11) Korotkov K.: http://www.korotkov.org/

-12 Fanti G.: Valutazione della risoluzione di immagini mediante analisi del modulo della funzione di trasferimento, VI Congresso Nazionale di Misure Meccaniche e Termiche, Desenzano del Garda, 12 - 14 Settembre 2005,
http://archimedes.ing.unibs.it/MMT/articoli/10-Risoluzione_Immagini.pdf